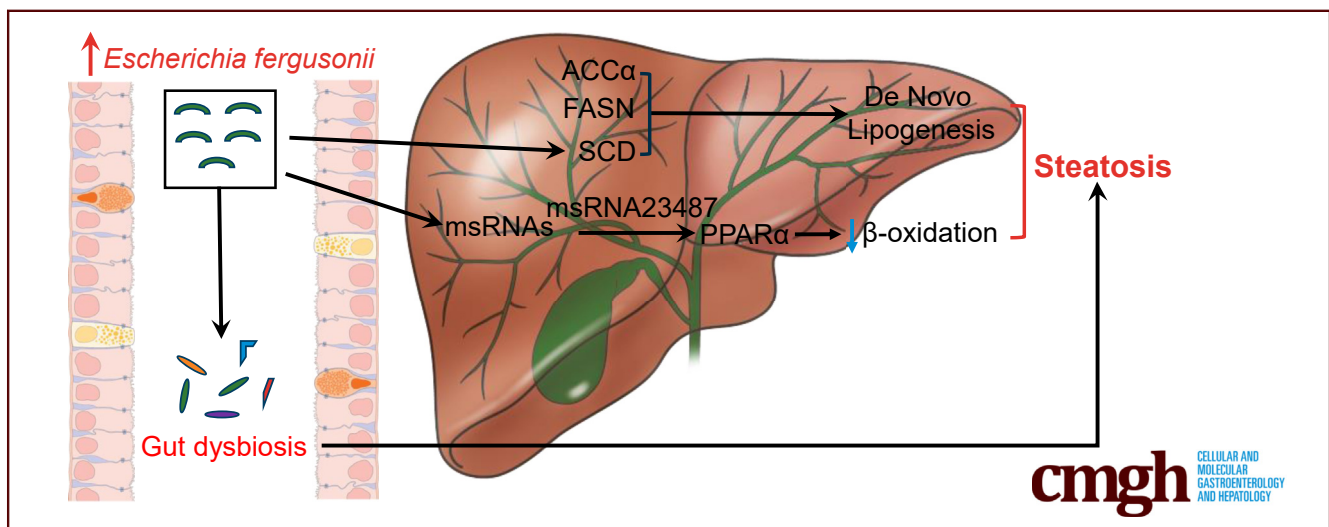


ORIGINAL RESEARCH

***Escherichia fergusonii* Promotes Nonobese Nonalcoholic Fatty Liver Disease by Interfering With Host Hepatic Lipid Metabolism Through Its Own msRNA 23487**

Feng-Zhi Xin,¹ Ze-Hua Zhao,¹ Xiao-Lin Liu,² Qin Pan,¹ Zi-Xuan Wang,¹ Lin Zeng,³ Qian-Ren Zhang,⁴ Lin Ye,⁵ Meng-Yu Wang,¹ Rui-Nan Zhang,¹ Zi-Zhen Gong,^{5,6,7} Lei-Jie Huang,¹ Chao Sun,¹ Feng Shen,¹ Lu Jiang,^{5,7,6} and Jian-Gao Fan^{1,6}

¹Department of Gastroenterology, Xinhua Hospital, Shanghai Jiao Tong University School of Medicine, Shanghai, China; ²Department of Gastroenterology, The First Affiliated Hospital of Soochow University, Suzhou, Jiangsu, China; ³CloudSeq Biotech, Inc, Shanghai, China; ⁴Department of Endocrinology, Xinhua Hospital, Shanghai Jiao Tong University School of Medicine, Shanghai, China; ⁵Shanghai Institute for Pediatric Research, Shanghai, China; ⁶Shanghai Key Lab of Pediatric Gastroenterology and Nutrition, Shanghai, China; ⁷Department of Pediatric Surgery, Xinhua Hospital, Shanghai Jiao Tong University School of Medicine, Shanghai, China

**SUMMARY**

Our study suggests that gut microbiota dysregulation and expansion of *Escherichia Shigella* are associated with the progression of nonobese nonalcoholic fatty liver disease. *Escherichia fergusonii* promotes the pathogenesis of steatohepatitis and fibrosis in nonobese rats by secreting msRNA 23487.

BACKGROUND & AIMS: Gut microbiota and microbial factors regulate the pathogenesis of nonalcoholic fatty liver disease (NAFLD) in patients with obesity and metabolic abnormalities, but little is known about their roles in nonobese NAFLD. Expansion of *Escherichia* is associated with NAFLD pathogenesis. We aimed to investigate the pathogenic role of *Escherichia fergusonii* and its products in the development of nonobese NAFLD.

METHODS: We characterized the intestinal microbiome signature in a cohort of NAFLD patients and healthy controls by 16S ribosomal RNA sequencing. The role of *E fergusonii* was

estimated in rats after 16 weeks of administration, and features of NAFLD were assessed. *E fergusonii*-derived microRNA-sized, small RNAs (msRNAs) were analyzed by deep sequencing.

RESULTS: We detected an expansion of *Escherichia Shigella* in NAFLD patients compared with healthy controls, and its increase was associated with disease severity independent of obesity. *E fergusonii*, a member of the genus *Escherichia*, induced the development of nonobese NAFLD characterized by hepatic steatosis and hepatocyte ballooning in rats without obesity. It disturbed host lipid metabolism by inhibiting hepatic lipid β -oxidation and promoting de novo lipogenesis. We also showed that *E fergusonii* caused the development of hepatic inflammation and fibrosis in a sizable fraction of animals at an advanced stage of NAFLD. Mechanistically, *E fergusonii*-derived msRNA 23487 down-regulated host hepatic peroxisome proliferator-activated receptor α expression, which could contribute to lipid accumulation in the liver.

CONCLUSIONS: These results suggest that *E fergusonii* promotes the pathogenesis of steatohepatitis and fibrosis in nonobese rats by secreting msRNA 23487, and it might be a potential biomarker for predicting steatohepatitis in nonobese

NAFLD. (*Cell Mol Gastroenterol Hepatol* 2022;13:827–841; <https://doi.org/10.1016/j.jcmgh.2021.12.003>)

Keywords: Steatosis; Gut Microbiota; Lipid Metabolism; Peroxisome Proliferator-Activated Receptor α .

Nonalcoholic fatty liver disease (NAFLD) is a metabolic stress-induced liver injury that is closely related to genetic susceptibility and insulin resistance in the absence of alcohol consumption. Currently, NAFLD has become the second-leading liver disease among patients awaiting liver transplantation in the United States.¹ The spectrum of NAFLD ranges from simple steatosis (or nonalcoholic fatty liver, NAFL) to nonalcoholic steatohepatitis (NASH), with the development of fibrosis, cirrhosis, and, finally, hepatocellular carcinoma.² NAFLD is seen commonly in patients with metabolic abnormalities associated with obesity, such as dyslipidemia, type II diabetes, and metabolic syndrome.³ Importantly, NAFLD has been reported in nonobese individuals based on liver biopsy, particularly in Asians.⁴ Studies have suggested that the incidence of NASH and fibrosis does not differ between obese and nonobese NAFLD patients.⁵ Considering the clinical significance and prevalence of nonobese NAFLD, studies are needed to understand its pathogenesis to identify high-risk patients and manage their metabolic profile.

A growing body of evidence suggests an intricate linkage between the gut microbiome and the pathogenesis of NAFLD.⁶ The gut microbiome is a diverse microbial community comprising trillions of bacteria, fungi, viruses, archaea, and protists that encode more functional genes than the human genome.⁶ In the past decade, compositional changes in the gut microbiota and its metabolites, such as short-chain fatty acids, branched-chain amino acids, indoles, and secondary bile acids have been reported in patients and animal studies in NAFLD.^{6,7} Zhu et al⁸ compared the gut microbiota of healthy, obese, and NASH patients. *Escherichia* was the only abundant genus that differed between obese and NASH patients, suggesting a possible role of *Escherichia* in driving NASH progression independent of obesity. Similar to eukaryotic cells, prokaryotes also can produce microRNA-sized, small RNAs (msRNAs) that play important roles in communicating between bacteria and hosts.⁹ In the current study, we investigated the role of *Escherichia fergusonii* and its product msRNA 23487 in the pathogenesis of nonobese NAFLD in rats.

Results

Expansion of *Escherichia_Shigella* Was Associated With NAFLD Severity

To determine whether NAFLD and NASH are associated with an altered composition of gut microbiota, we performed 16S ribosomal RNA (rRNA) gene sequencing using fecal samples from healthy controls (n = 25) and NAFLD patients (n = 29). Overall, the bacterial richness within the groups based on the Sobs estimator was reduced significantly in NAFLD patients compared with healthy controls. The Sobs estimator in patients with overweight or obesity,

with NAFL or NASH, and with or without fibrosis also was decreased significantly compared with healthy controls (Figure 1A). Furthermore, partial least-squares discrimination analysis showed a significant change in the composition of the gut microbiota in NAFLD patients compared with healthy controls (Figure 1B). In different subgroups of NAFLD (patients with overweight or obesity, with NAFL or NASH, with or without fibrosis), we also detected a clustering difference between NAFLD subgroups and controls (Figure 1B). Moreover, the relative abundance at the phylum or genus levels showed alterations in the gut microbiota profile in NAFLD patients. Finally, the relative abundance of Proteobacteria (Figure 1C and D) and the Firmicutes:Bacteroidetes ratio were increased in the NAFLD group compared with healthy controls (2.02 vs 1.00) (Figure 1E).

One substantial difference that we observed was an increase in the proportion of *Escherichia_Shigella*, a member of Proteobacteria, in NAFLD patients (Figure 1D). Moreover, the relative abundance of *Escherichia_Shigella* was increased significantly in nonobese NAFLD patients compared with healthy controls (Figure 1F), suggesting a possible pathogenic role of *Escherichia_Shigella* in nonobese NAFLD development. Spearman correlation analysis (Figure 1G) showed that the relative abundance of *Escherichia_Shigella* was associated with the development of hepatic inflammation (adjusted $R^2 = 0.244$; $P < .0001$) and fibrosis (adjusted $R^2 = 0.309$; $P < .0001$).

E fergusonii Altered the Gut Microbiome Profile in Rats

To date, 7 species have been identified in the genus *Escherichia*, among which *E fergusonii* is a rare pathogen that can infect both human beings and animals.¹⁰ To determine the effect of *E fergusonii* on the gut microbiome profile and biological functions, we treated rats with *E fergusonii* daily for 16 weeks by oral gavage. Daily administration was necessary because *E fergusonii* does not colonize rats (Figure 2A). We found that *E fergusonii* administration caused a shift in gut microbiota and tended to reduce the α -diversity under phylogenetic diversity_whole_tree measurement (Figure 2B). β -diversity based on principal coordinates and the unweighted pair-group method with arithmetic means analysis showed that the *E fergusonii* and control groups clustered differently (Figure 2C). Interestingly, *E fergusonii* administration increased the abundance

Abbreviations used in this paper: ALT, alanine aminotransferase; AST, aspartate aminotransferase; con, control; HDL-C, high-density lipoprotein cholesterol; HFHC, high-fat, high-cholesterol; LDL-C, low-density lipoprotein cholesterol; msRNA, microRNA-sized, small RNA; NAFL, nonalcoholic fatty liver; NAFLD, nonalcoholic fatty liver disease; NASH, nonalcoholic steatohepatitis; NC, negative control; PCR, polymerase chain reaction; PPAR α , peroxisome proliferator-activated receptor α ; rRNA, ribosomal RNA; sRNA, small RNA.

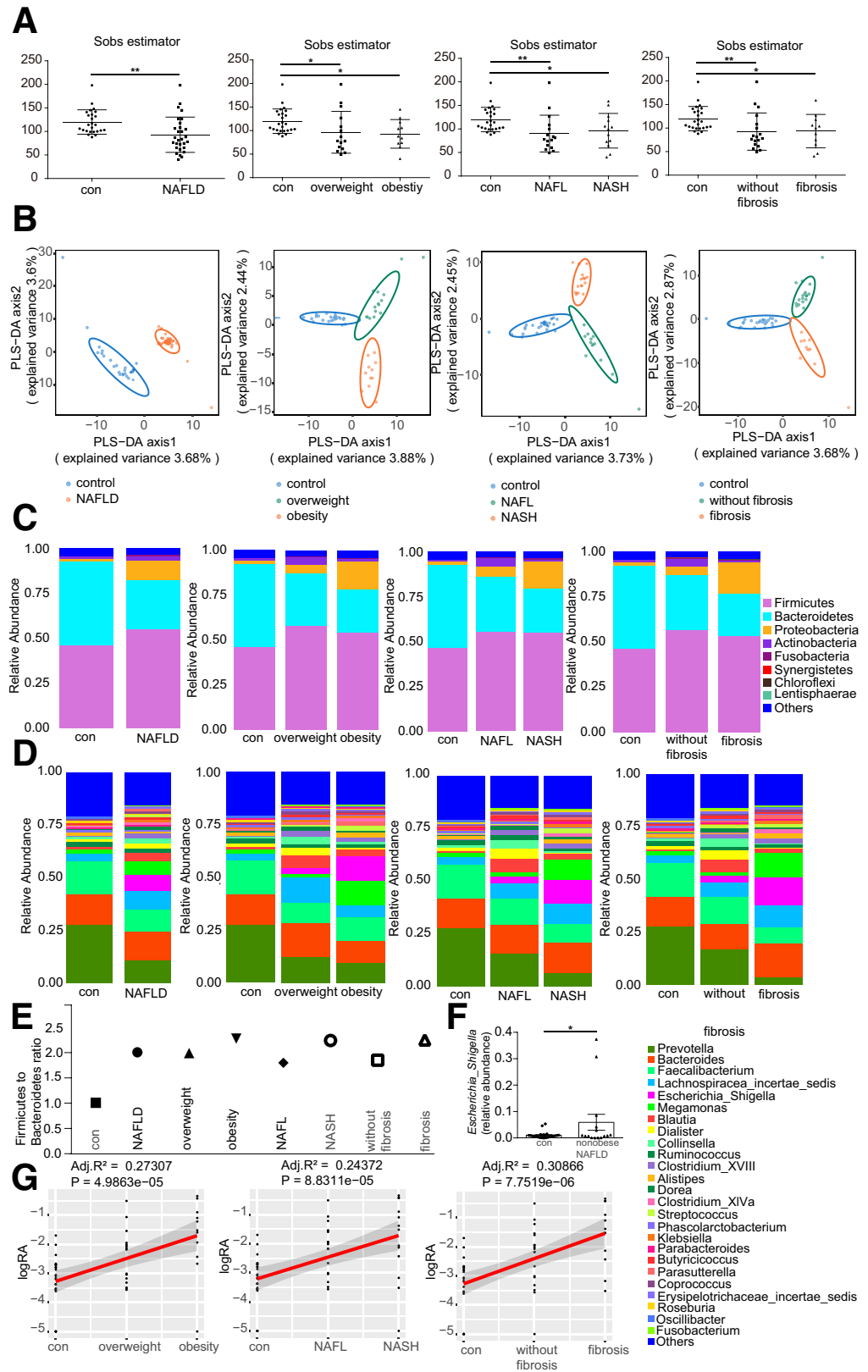


Most current article

© 2021 The Authors. Published by Elsevier Inc. on behalf of the AGA Institute. This is an open access article under the CC BY-NC-ND license (<http://creativecommons.org/licenses/by-nc-nd/4.0/>).

2352-345X

<https://doi.org/10.1016/j.jcmgh.2021.12.003>



of Proteobacteria (13.35-fold vs the control [con]+saline group) and decreased the abundance of Bacteroidetes (0.75-fold vs con+saline group) at the phylum level (Figure 2D).

Linear discriminant effect-size analysis was performed to identify the features most likely to account for differences among groups (Figure 2E). In addition, *E fergusonii* altered

gut microbiota functions based on Phylogenetic Investigation of Communities by Reconstruction of Unobserved States analysis. Pathways associated with metabolism, metabolic diseases, energy, amino acids, carbohydrate metabolism, and lipid metabolism were up-regulated with high-fat, high-cholesterol (HFHC) treatment, and the same trends were observed after *E fergusonii* administration. Importantly, pathways associated with lipid synthesis and metabolism also were dysregulated by *E fergusonii* (Figure 2F). These data indicate that *E fergusonii* disturbs host metabolic homeostasis by altering the gut microbiome profile, which may lead to the progression of NAFLD.

E fergusonii Induced Pathologic Features of Nonobese NAFLD in Rats

Next, we analyzed the effect of *E fergusonii* on hepatic pathologic features associated with NAFLD. Livers from the *E fergusonii* treatment group were larger in size and appeared pale in color compared with the con+saline group. We also detected lipid droplet accumulation, hepatomegaly, and hepatocellular ballooning in the *E fergusonii* group (Figure 3A). Steatosis and the hepatocellular ballooning score were significantly higher in the *E fergusonii* group than in the con+saline group (Figure 3B and C). Rats fed the HFHC diet showed a dramatic body weight gain after 16 weeks, while *E fergusonii* strongly aggravated liver lesions with no effect on body weight (Figure 3D). Increased hepatic triglyceride and total cholesterol levels further supported that *E fergusonii* disturbed host hepatic lipid metabolism (Figure 3F). Finally, the percentages of liver index and epididymal fat were increased significantly in the *E fergusonii* group (Figure 3E). All of these findings suggested that *E fergusonii* induced the development of nonobese NAFLD characterized by hepatic steatosis and hepatocellular ballooning without causing obesity in rats.

E fergusonii Induced Steatohepatitis in a Proportion of Animals

NASH is the most serious form of NAFLD, characterized by hepatic inflammation and fibrosis as the result of a second hit.¹¹ We therefore explored whether *E fergusonii* administration induced hepatic inflammation and fibrosis in rats. As we expected, the HFHC group showed marked inflammatory and fibrotic phenotypes by histology (Figure 4A and B). Liver injury assessed by serum levels of alanine aminotransferase (ALT) and aspartate aminotransferase (AST) was increased significantly in the HFHC diet group (Figure 4C). Reactive oxygen species-related cytoplasmic subunits, such as *p47phox* and *p67phox*, were up-regulated in the HFHC diet group, while the toxic substance binding protein *Ass1* was decreased with the HFHC diet (Figure 4D). Furthermore, quantification of Masson trichrome and Sirius red staining showed that the HFHC diet caused fibrosis in 70% of animals that were fed that diet. Specifically, 7 of 10 rats displayed a fibrosis score greater than 1 (Figure 4A and B). Among all animals in the *E fergusonii* group, 20% (2 of 10) developed hepatic inflammation, and 20% (2 of 10) showed sinus fibrosis (fibrosis score 1) with scattered

inflammatory cell infiltration (Figure 4A and B). We confirmed that rats that developed either inflammation or fibrosis were different animals. Therefore, 40% (4 of 10) of rats in the *E fergusonii* group developed advanced-stage NAFLD. Aside from increased AST levels (Figure 4C), ALT levels tended to increase with *E fergusonii* administration, although the increase was not statistically significant. Taken together, these data showed that *E fergusonii* induced steatohepatitis in a sizable fraction of rats.

E fergusonii Dysregulated Host Lipid Metabolism

To understand the mechanisms underlying the increased hepatic lipid accumulation, we next measured biochemical parameters critically involved in fatty acid and cholesterol metabolism. The HFHC diet significantly increased the levels of triglycerides (Figure 5A), cholesterol (Figure 5B), fasting blood glucose level (Figure 5C), low-density lipoprotein cholesterol (LDL-C) (Figure 5E), homocysteine (Figure 5F), and total bile acids (Figure 5G) compared with those of the con+saline group, while the high-density lipoprotein cholesterol (HDL-C) level was decreased (Figure 5D). In comparison, *E fergusonii* increased serum triglyceride, cholesterol, fasting blood glucose, LDL-C, homocysteine, and total bile acid levels, while reducing HDL-C levels (Figure 5A–G).

Next, we evaluated gene expression related to lipid metabolism in the liver. As shown in Figure 5H, *E fergusonii* increased the expression of genes associated with de novo lipogenesis, such as *Srebp1c*, *Scd*, *Fasn*, and *Acc*. Furthermore, *E fergusonii* significantly reduced ligand-activated transcription factor peroxisome proliferator-activated receptor α (*Ppara*) expression, a master regulator of fatty acid uptake, β oxidation, ketogenesis, bile acid synthesis, and triglyceride turnover.¹² Genes associated with fatty acid oxidation (*Cpt1a*, *Fabp1*, *Acadl*, and *Acadvl*) and lipid transport (*Acs1* and *Fatp2*) also were down-regulated with *E fergusonii* treatment or HFHC diet (Figure 5I). These data suggest that *E fergusonii* disturbs host hepatic lipid metabolism by inhibiting fatty acid oxidation and enhancing lipid de novo lipogenesis.

msRNA Sequencing Analysis of *E fergusonii*

To understand the mechanisms underlying the hepatic lipid accumulation caused by *E fergusonii*, we next focused on *E fergusonii*-derived products. Recently, bacteria-derived msRNAs have been reported to regulate host physiological functions.¹³ To characterize the msRNA profile of *E fergusonii* and investigate whether it affected host lipid metabolism, we performed deep sequencing analysis on *E fergusonii*. As shown in Figure 6A, most reads were detected between 15 and 33 nt, which was the typical size of miRNAs. A list of msRNAs with a high miRDeep2 score or cloning copy number reads is summarized in Table 1. Among all msRNAs identified, msRNA 15919 and msRNA 23487 showed the highest miRDeep2 score and cloning copy number. Moreover, enrichment analysis of biological processes showed that msRNAs from *E fergusonii* had an appreciable impact on host hepatic metabolic processes,

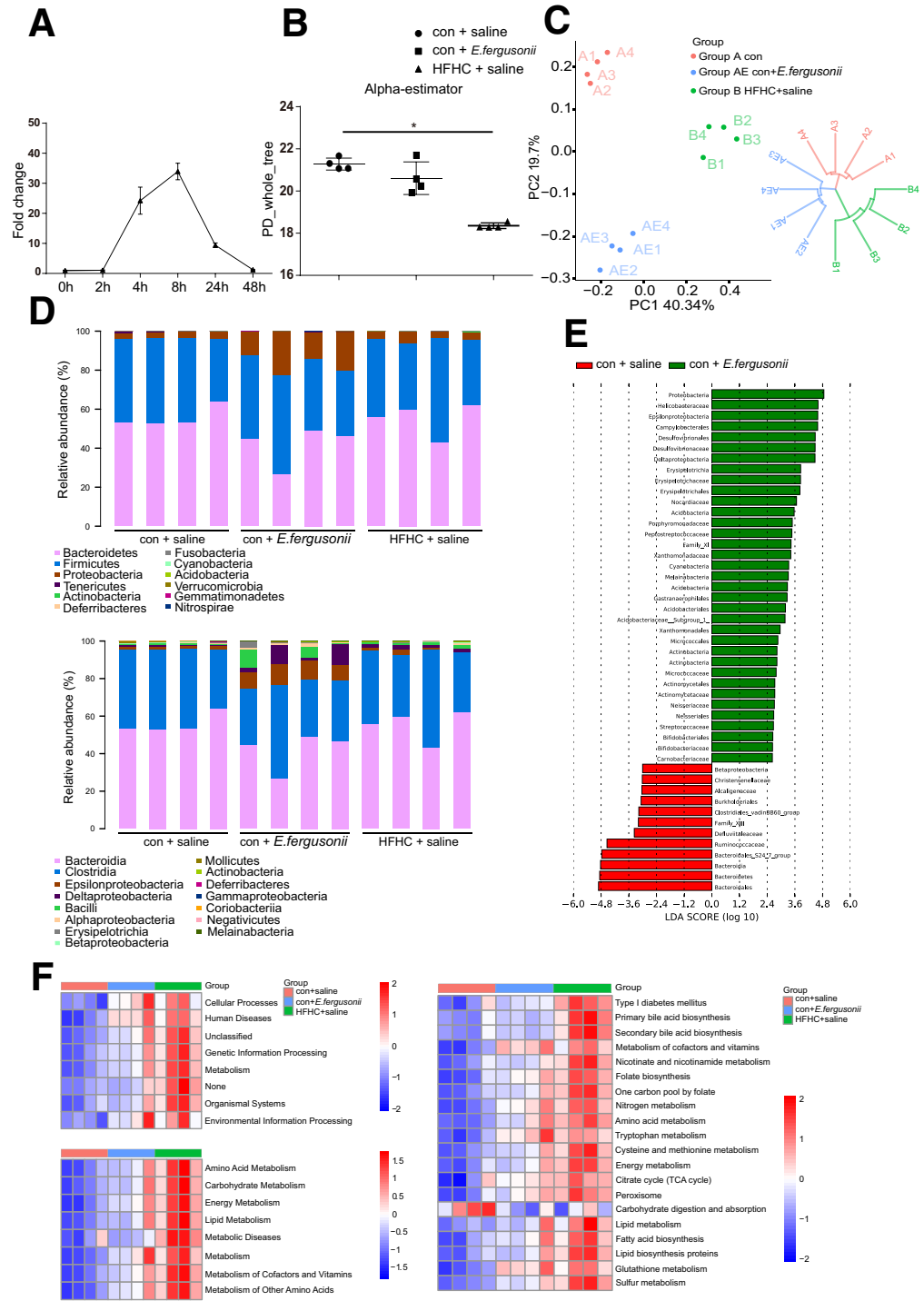


Figure 2. *E. fergusonii* altered the gut microbiome composition and functions. (A) *E. fergusonii* was detected in feces from rats gavaged with *E. fergusonii* (3×10^9 colony-forming units), assessed by quantitative PCR. $n = 6$ per group. (B) Bacterial richness was estimated based on the Sobs estimator in rats from the con+saline, con+*E. fergusonii*, and HFHC+saline groups. (C) β -diversity in rats from the different groups. (D) Relative abundance of bacteria at the phylum (upper) and class (lower) levels in rats from different groups. (E) Linear discriminant analysis effect size analysis between the con+saline and con+*E. fergusonii* groups. (F) Phylogenetic Investigation of Communities by Reconstruction of Unobserved States analysis predicted gene functions in rats from different groups. * $P < .05$. LDA, linear discriminant analysis; PC, principal coordinate; PD, phylogenetic diversity; TCA, tricarboxylic acid cycle.

including lipid metabolism (Figure 6B). According to the number of reads and the enrichment results, msRNA 23487, msRNA 14034, msRNA 3940, msRNA 2070, msRNA 285, and msRNA 21754 were selected for further analysis. As shown in Figure 6D, we predicted the secondary structures of the precursor hairpin of the msRNAs. Furthermore, msRNA expression levels were verified by quantitative polymerase chain reaction (PCR) (Figure 6C).

Among all msRNAs, msRNA 23487 had the highest expression compared with other msRNAs after *E. fergusonii* treatment. Although all the msRNAs mentioned earlier were up-regulated after *E. fergusonii* administration, msRNA 23487 showed the highest increase. To confirm that msRNA 23487 was secreted from *E. fergusonii*, we mapped the whole sequence of msRNA 23487 against the database nucleotide collection (nt) using the web-based

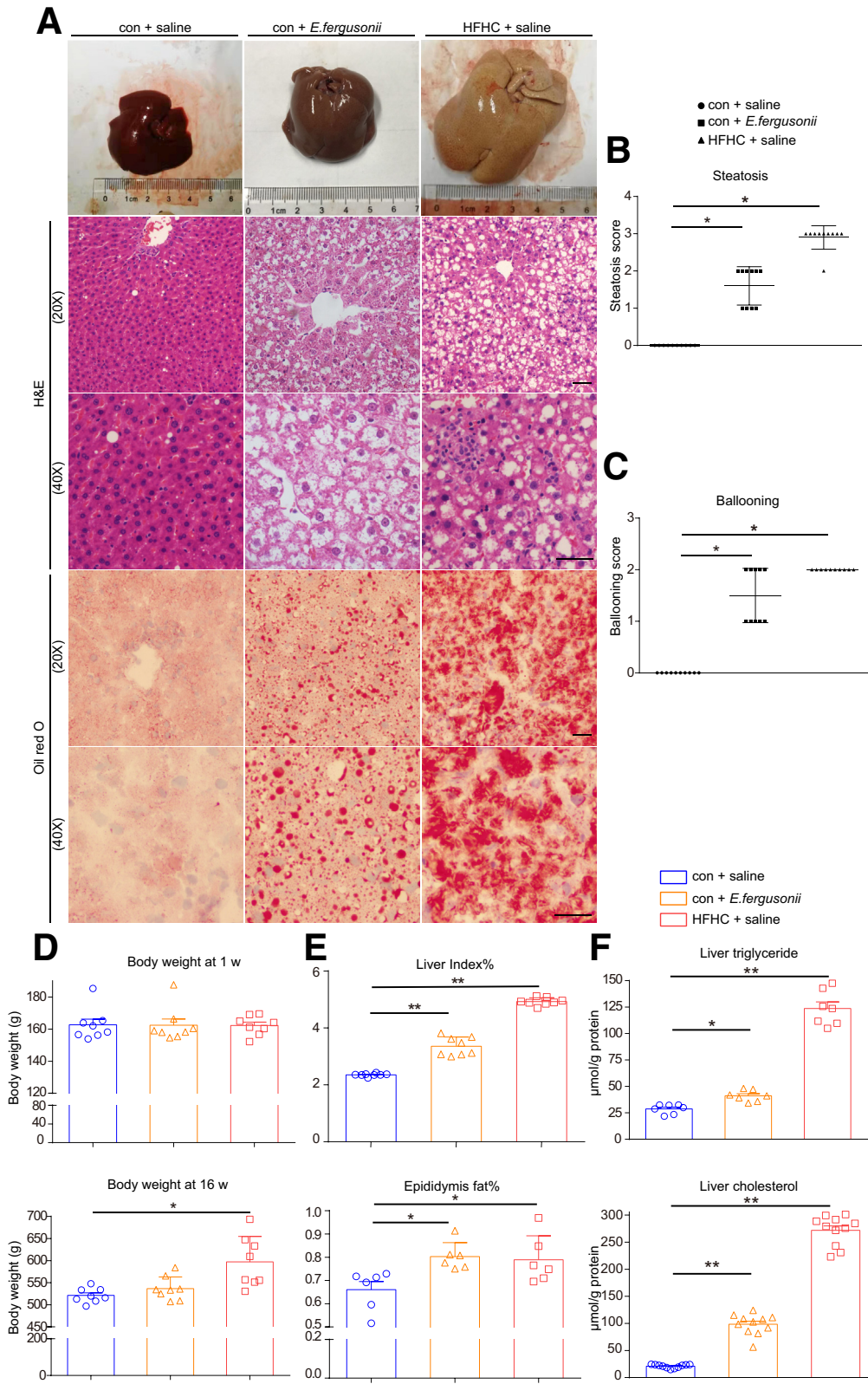
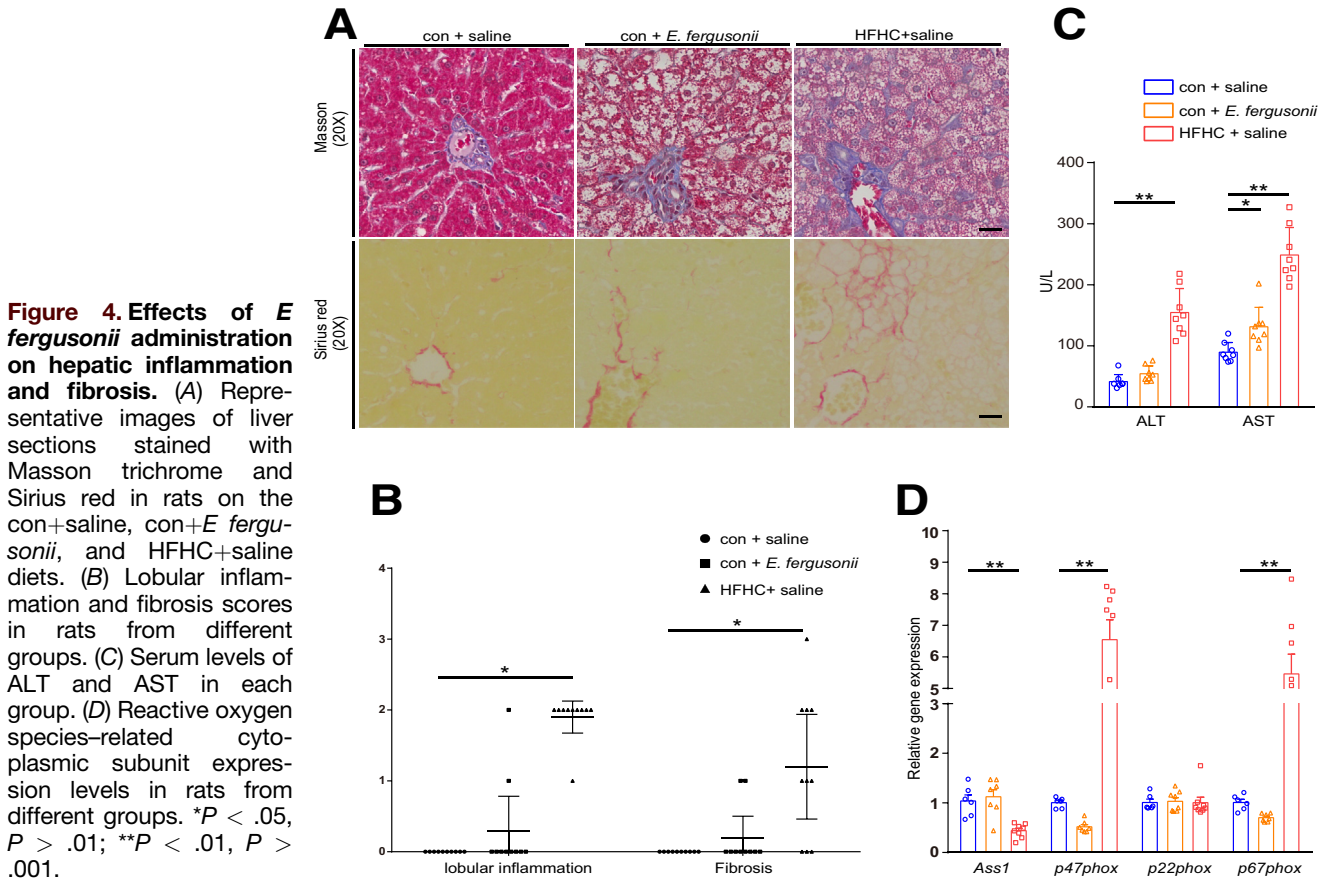


Figure 3. *E. fergusonii* induced hepatic steatosis and hepatocellular ballooning. (A) Representative images of liver, H&E, and Oil Red O staining in rats on the con+saline, con+*E. fergusonii*, and HFHC+saline diets. (B) Steatosis score and (C) hepatocyte ballooning score in rats from different groups. (D) Body weight at 1 week and 16 weeks in each group. (E) Liver index (%) and epididymis fat (%) in rats from different groups. (F) Liver triglyceride levels and cholesterol in rats from different groups. * $P < .05$, $P > .01$; ** $P < .01$, $P > .001$.

NCBI tool Nucleotide BLAST (<https://blast.ncbi.nlm.nih.gov/Blast.cgi>). As we expected, msRNA 23487 was aligned to *E. fergusonii* ATCC 35469 with 100% query cover

(Table 2). Taken together, *E. fergusonii* had a unique msRNA signature that may function to disturb host lipid metabolism.



msRNA 23487 From *E fergusonii* Promoted Lipid Accumulation by Regulating PPAR α

To test whether the increased expression of msRNA 23487 is involved in regulating host lipid metabolism, we first examined its target genes predicted by miRanda software.¹⁴ Interestingly, PPAR α was predicted to be one of msRNA 23487 target genes, which was confirmed by a decreased PPAR α protein level in rat livers after *E fergusonii* treatment (Figure 7A). We next evaluated the effect of msRNA 23487 on PPAR α levels by transfecting Huh7 and HepG2 cells with msRNA 23487 mimic or the corresponding negative control (NC). The expression level of msRNA 23487 was increased significantly after transfection with the msRNA 23487 mimic. There was no change in the messenger RNA levels of *Ppara*, while the protein levels showed a significant reduction when Huh7 and HepG2 cells were transfected with the msRNA 23487 mimic (Figure 7B and C).

To further evaluate the function of msRNA 23487 on host hepatic lipid metabolism in vitro, we transfected Huh7 and HepG2 cells with NC or msRNA 23487 mimic cocultured with 0.3 mmol/L palmitic acid solution. As expected, cells transfected with the msRNA 23487 mimic showed more lipid accumulation than NC cells, as shown by Oil Red O staining and triglyceride assays (Figure 7D and E). Taken together, msRNA 23487 promoted liver lipid accumulation by down-regulating PPAR α expression, possibly at the post-transcriptional level.

Discussion

The role of the gut microbiome–liver axis in the pathogenesis of NAFLD has been studied predominantly in patients with metabolic abnormalities. However, the impact and precise mechanisms of gut microbiota in nonobese NAFLD are poorly understood. Herein we provide an example of the pathogenic effect of *E fergusonii* on inducing the development of nonobese NAFLD in rats. We also proposed a novel mechanism by which *E fergusonii* regulated host lipid metabolism by producing msRNA 23487, which down-regulated PPAR α expression at the protein level.

There is a growing body of evidence suggesting that an overall decrease in microbial diversity and the expansion of selected bacterial families are associated with NAFLD pathogenesis.⁶ Among them, the most widely known contributors are *Firmicutes* and *Bacteroidetes*, the 2 major components of the human gut microbiota.¹⁵ Increased *Firmicutes* levels with decreased *Bacteroidetes* levels have been detected in a number of metabolic-related diseases including NAFLD.^{16,17} Consistent with previous findings,^{7,18} we found an increased *Firmicutes*:*Bacteroidetes* ratio and an increased abundance of *Proteobacteria* in patients with NAFLD, and their levels were higher in patients with obesity, inflammation, and fibrosis. Moreover, we found that *Escherichia Shigella* was expanded in NAFLD patients, and its abundance was correlated significantly with NAFLD severity. Consistent with our study, Zhu et al⁸ also

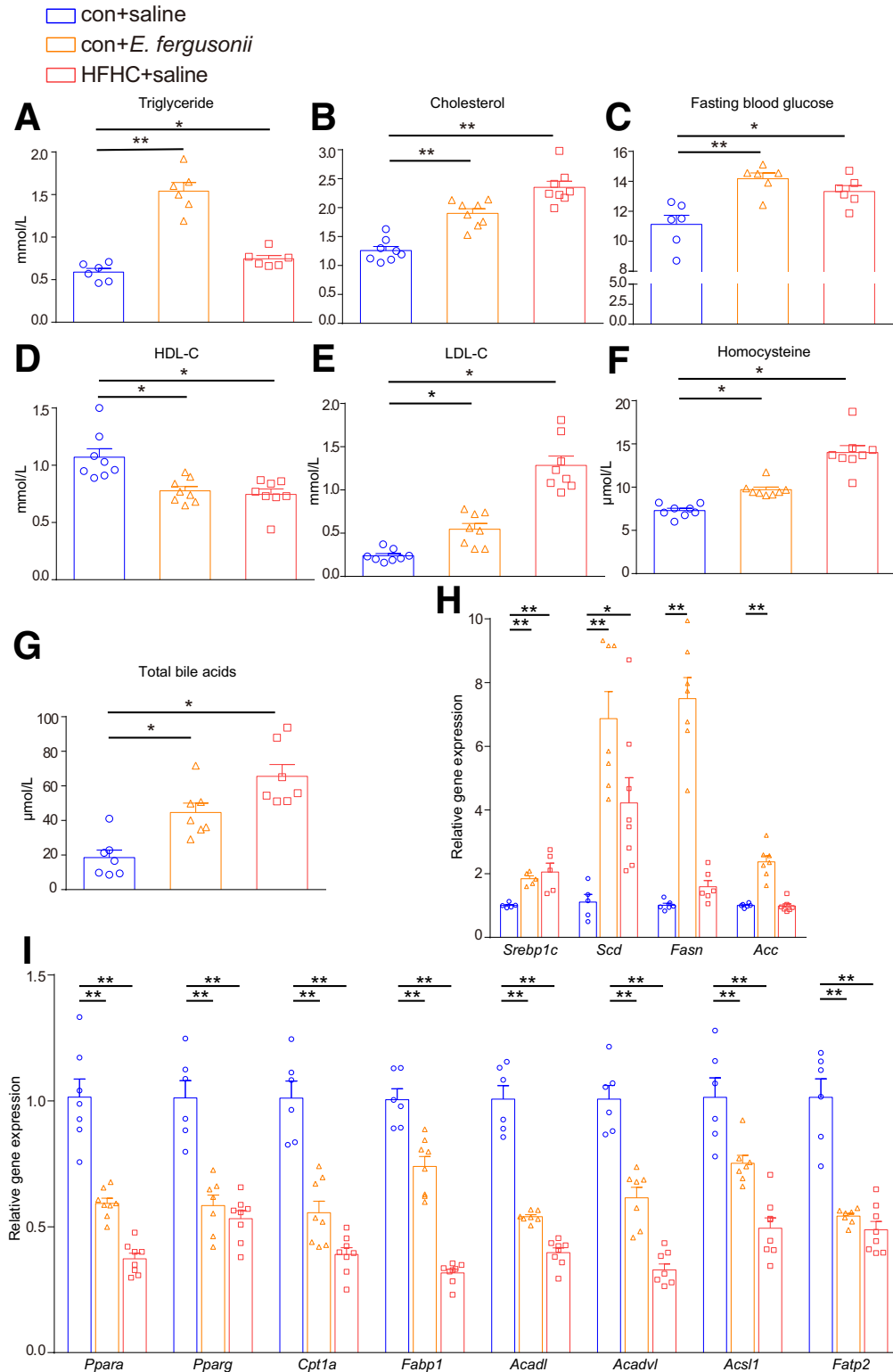


Figure 5. *E. fergusonii* disturbed the serum lipid profile and hepatic lipid metabolism. (A–G) Serum triglyceride, cholesterol, fasting blood glucose, HDL-C, LDL-C, homocysteine, and total bile acid levels in the con+saline, con+*E. fergusonii*, and HFHC+saline groups. (H) Expression levels of *Srebp1c*, *Scd*, *Fasn*, and *Acc* in rats from different groups. (I) Expression levels of *Ppara*, *Pparg*, *Cpt1α*, *Fabp1*, *Acadl*, *Acadvl*, *Acs1*, and *Fatp2* in rats from different groups. * $P < .05$, $P > .01$; ** $P < .01$, $P > .001$.

confirmed that *Escherichia* was the only genus that was significantly different between obese and NASH patients, suggesting a pathogenic role of *Escherichia* in NASH progression independent of obesity. There are 7 identified

species in the genus *Escherichia*, of which *E. fergusonii* initially was isolated in human blood samples in 1985.¹⁹ Because *E. fergusonii* and *E. coli* are congeneric species with 64% similarity in DNA hybridization, they could be

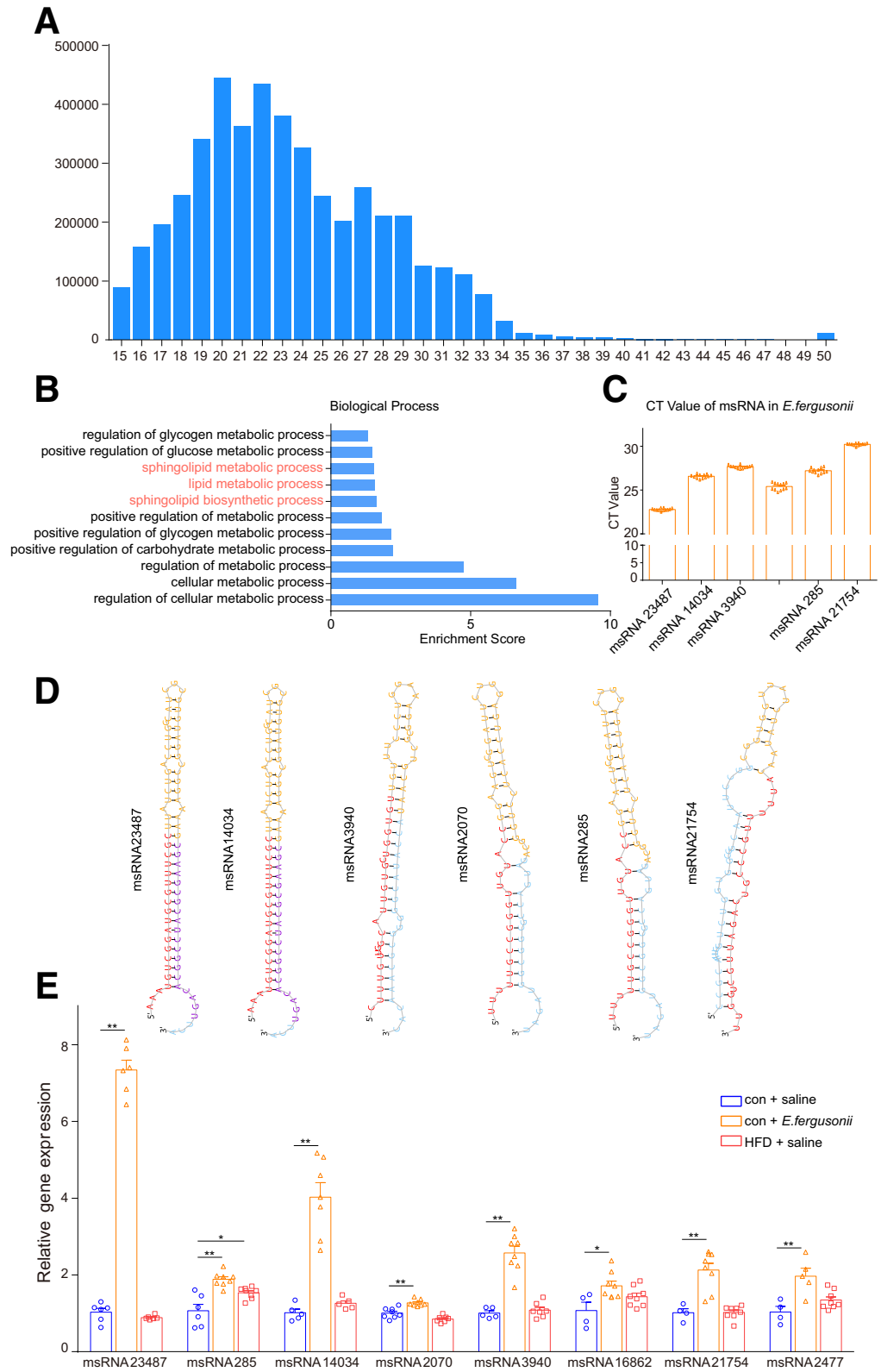


Figure 6. Deep sequencing analysis of *E. fergusonii*. (A) Identification of msRNAs in *E. fergusonii*. (B) Biological process of *E. fergusonii*-derived msRNAs. (C) cycle threshold values of msRNAs in *E. fergusonii*. (D) Secondary structure prediction of *E. fergusonii*-derived msRNAs. (E) Expression levels of *E. fergusonii*-derived msRNAs in livers from the con+saline, con+*E. fergusonii*, and HFD+saline groups. * $P < .05$, $P > .01$; ** $P < .01$, $P > .001$.

difficult to differentiate using PCR methods.²⁰ To solve this problem, we used both PCR and lactose-negative experiments to differentiate *E. fergusonii* from *E. coli* before the animal experiment (data not shown).

Although obesity is a common clinical phenotype associated with NAFLD, a nonobese population without obvious risk factors also can develop NAFLD. In our study, we found that administration of *E. fergusonii* alone could

Table 1. List of msRNAs With High Numbers of Reads or High miRDeep2 Scores

msRNA name	miRDeep2 score	Reads, n	msRNA sequence	Length	Validation
msRNA 15919	63,000	124,422	AUUUGUGGAGCCCAUCAACC	20	qPCR
msRNA 23487	1100	2168	AAAUGUCGGAGUCGUUUCGC	20	qPCR
msRNA 17782	180	364	GACGACAAAUCGCUGUUUCUUGAC	24	
msRNA 10285	100	218	CUGCGAUCUGUUAUACUC	1	
msRNA 14555	96	194	UUGUCGCUGCCGUCAGC	17	
msRNA 9728	94	189	AGUUCGUCGUCGUGAAUU	18	qPCR
msRNA 285	1	558	UUUGCCACGGAACGGUCUG	19	qPCR
msRNA 9506	0.6	4453	UUAACGAUGACGGUCUGUUUUACG	25	
msRNA 3940	0.6	184	CUUUGUUGGCAUUGUCUGGUGU	23	qPCR
msRNA 14034	0.5	439	CUCGACGAUGCCGGCAAUGGCCUG	25	qPCR
msRNA 21754	0.4	176	AUUUUUGCCGUCAGAUUGCUGGUU	25	qPCR
msRNA 25190	0.2	2871	UAUUGCUGCUGUUGCGCC	19	

qPCR, quantitative PCR.

induce the development of nonobese NAFLD, characterized by hepatic steatosis and hepatocellular ballooning without causing body weight gain in rats. In particular, hepatic triglyceride levels were induced significantly by *E. fergusonii* administration, indicating a potential role in disturbing lipid metabolism to promote lipid accumulation, possibly through regulating the PPAR α signaling pathway. Furthermore, we detected that a sizable fraction of animals developed advanced NAFLD, characterized by hepatic inflammation and fibrosis. These histopathologic characteristics indicated that 16 weeks of *E. fergusonii* administration to rats induced hepatic pathology indicative of nonobese NAFLD that potentially can progress to NASH. It is possible that a higher dose or longer administration time of *E. fergusonii* may cause a higher proportion of NASH development.

It is widely known that the gut microbiome contributes to NAFLD pathogenesis by producing microbial metabolites, such as bile acids, short-chain fatty acids, branched-chain

amino acids, lipopolysaccharides, and indoles.⁶ In our study, we proposed a novel mechanism by which *E. fergusonii* promotes lipid accumulation by secreting msRNAs. The existence of msRNAs has been shown in *E. coli* and *Streptococcus mutans* by using a deep sequencing approach.²¹ To investigate whether *E. fergusonii* exerts its functions via msRNAs, we performed deep sequencing to characterize the msRNA profile of *E. fergusonii* in the context of NAFLD. We identified msRNA 23487 as the most up-regulated msRNA after *E. fergusonii* administration, and msRNA 23487 secreted by *E. fergusonii* regulated host lipid metabolism by down-regulating hepatic PPAR α expression.

Our study can be improved by using third-generation sequencing to characterize bacterial signatures in healthy controls and NAFLD patients, which will provide higher resolution of microbial taxonomy compared with our current 454 pyrosequencing technology.²² Studies are needed to confirm the abundance of *E. fergusonii* in nonobese NAFLD patients, and to further investigate whether a longer

Table 2. Basic Local Alignment Search Tool Nucleotide (BLASTn) Results for msRNA 23487 Against the Nucleotide Collection (nt) Database With 100% Query Cover

Description	Maximum score	Total score	Query cover	E value	Percentage identity	Accession
<i>E. fergusonii</i> ATCC 35469 chromosome, complete genome	139	139	100%	3.00E-30	100.00%	NC_011740.1
<i>E. fergusonii</i> strain ATCC 35473 chromosome, complete genome	134	134	100%	1.00E-28	98.67%	NZ_CP042942.1
<i>E. fergusonii</i> strain ATCC 35470 chromosome, complete genome	134	134	100%	1.00E-28	98.67%	NZ_CP042946.1
<i>E. coli</i> strain EC42405 chromosome, complete genome	134	134	100%	1.00E-28	98.67%	NZ_CP043414.1
<i>E. coli</i> strain 2013C-4282 chromosome, complete genome	134	134	100%	1.00E-28	98.67%	NZ_CP027579.1
<i>E. coli</i> strain EC42405 chromosome, complete genome	134	134	100%	1.00E-28	98.67%	CP043414.1

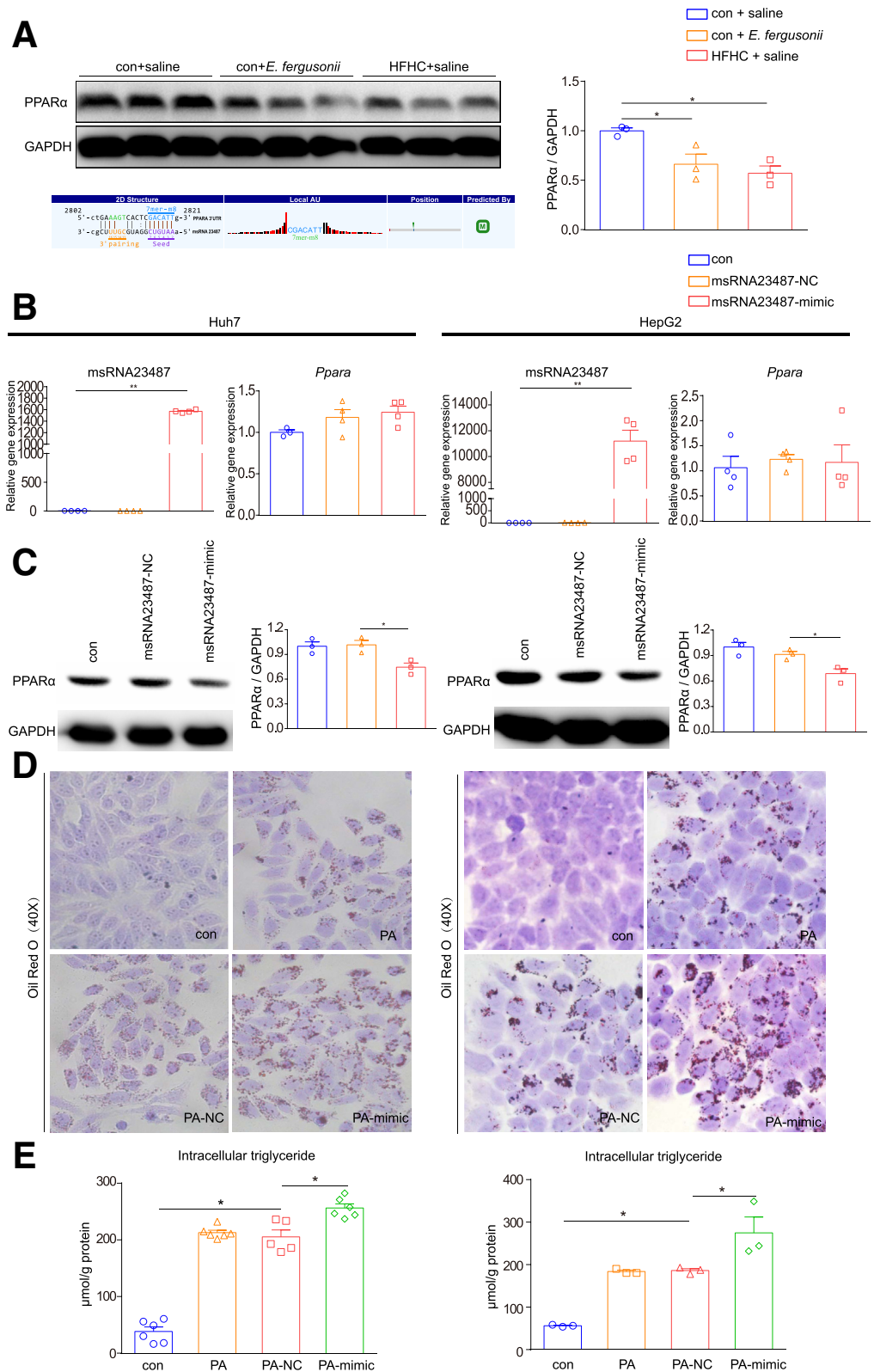


Figure 7. msRNA 23487 from *E. fergusonii*-induced lipid accumulation by interacting with PPAR α . (A) Western blot for PPAR α protein in liver. Glyceraldehyde-3-phosphate dehydrogenase (GAPDH) is shown as a loading control for liver protein (upper panel); binding sites of PPAR α messenger RNA with msRNA 23487 predicted by miRanda software (lower panel). (B) Expression levels of msRNA 23487 and *PPAR α* after transfection with msRNA 23487 NC or mimic in Huh7 and HepG2 cell lines. (C) PPAR α protein levels after transfection with msRNA 23487 NC or mimic in Huh7 and HepG2 cell lines. (D) Oil Red O staining after transfection with msRNA 23487 NC or mimic in Huh7 and HepG2 cell lines. (E) Intracellular triglyceride levels after transfection with msRNA 23487 NC or mimic in Huh7 and HepG2 cell lines. * $P < .05$, $P > .01$; ** $P < .01$, $P > .001$.

administration or higher doses will cause an advanced stage of NAFLD in a higher proportion of animals. In addition, studies are needed to validate the effects of *E. fergusonii* in germ-free mice or mice treated with antibiotics to reduce

the amount of intestinal bacteria. Last, a recent study from Tu et al²³ suggested that mice fed with a HFHC cholate diet developed nonobese NAFLD in 3 weeks. Including the HFHC cholate group in our study would be informative to evaluate

the role of *E fergusonii* in the pathogenesis of nonobese NAFLD.

In summary, we have shown that *Escherichia Shigella* was increased in NAFLD patients, and its expansion was associated with disease aggravation independent of obesity. *E fergusonii*, an important species in the *Escherichia* genus, induced the development of nonobese NAFLD in rats, which is characterized by hepatic steatosis and hepatocyte ballooning with partial development of fibrosis and inflammation without weight gain. By identifying msRNA 23487 as a regulator of PPAR α expression, we proposed a new mechanism by which *E fergusonii* regulates host lipid metabolism in nonobese NAFLD. Targeting *E fergusonii* and its product msRNA 23487 might contribute to the clinical management of the disease.

Materials and Methods

Patient Cohorts

A total of 54 subjects were included in this study, of which 29 subjects had biopsy-proven NAFLD and 25 subjects were healthy controls. There was no significant difference in sex or age between the NAFLD group and the healthy controls. In the NAFLD group, 15 subjects were diagnosed with overweight and 11 subjects were diagnosed as obesity according to the Chinese diagnostic criteria for obesity.²⁴ Furthermore, 16 subjects were diagnosed with NAFL and 13 subjects were diagnosed with NASH; 18 subjects had fibrosis, and 11 subjects had no fibrosis based on the steatosis, activity, and fibrosis score.²⁵ All subjects provided informed consent for participation before enrollment. The protocol was approved by the Ethics Committee of Xinhua Hospital affiliated with Shanghai Jiao Tong University School of Medicine.

Animal Experiments

E fergusonii (ATCC 35469) was obtained from Guangdong Culture Collection Center (China). *E fergusonii* for oral administration was obtained from subcultured bacterial cryopreservation in Luria-Bertani broth and suspended in sterile saline at a concentration of 3×10^9 colony-forming units/mL for subsequent animal experiment use.

Specified pathogen-free male Sprague Dawley rats (Sipurbec Laboratory Animal Co, Ltd, Shanghai, China) were kept in a controlled environment with free access to water and a standard chow diet. After adaptive feeding for 7 days, rats were assigned to 3 groups according to the diet type and bacterial intervention ($n = 10$ per group): chow diet with saline (con+saline), chow diet with *E fergusonii* (con+*E fergusonii*), and a HFHC diet with saline (HFHC+saline). The HFHC diet contains 88% standard diet, 10% lard, and 2% cholesterol. Saline (1 mL) containing 3×10^9 colony-forming units of *E fergusonii* was gavaged daily, starting from day 1 of the con+*E fergusonii* group. The con+saline and HFHC+saline groups were fed 1 mL of sterile saline. After 16 weeks, all rats were fasted overnight and killed to collect serum, liver, intestine, and fecal samples for the following analysis. All animal experiments were approved by the Institutional Animal Care and Use

Committee of Xinhua Hospital affiliated with Shanghai Jiao Tong University School of Medicine and were conducted in accordance with the National Research Council Guide for Care and Use of Laboratory Animals.

Biochemical Assays

Serum ALT, AST, alkaline phosphatase, fasting blood glucose, HDL-C, LDL-C, total bile acids, homocysteine, total triglyceride, and total cholesterol were measured by a fully automatic biochemical analyzer (SYSMEX, Kobe, Japan) with 6–8 samples per experimental group according to the manufacturer's instructions. Hepatic and cellular triglycerides and cholesterol were evaluated using triglyceride and cholesterol assay kits (E1013-105 and E1015-105; Applygen Technologies, Inc, Beijing, China). The final concentrations of triglycerides were corrected according to the protein concentration.

Histologic Analysis of Liver Tissues

Formalin-fixed tissue samples were embedded in paraffin and stained with H&E for morphologic observation. Masson trichrome staining and Sirius Red staining were performed to evaluate fibrosis. The steatosis, activity, and fibrosis score was evaluated based on histologic features. Frozen sections were embedded in optimal cutting temperature compound and stained with Oil Red O to analyze lipid accumulation.

Real-Time Quantitative PCR

Total RNA from liver or cells was extracted using TRIzol (TaKaRa, Tokyo, Japan), and complementary DNA was generated using PrimeScript RT master mix (TaKaRa, Tokyo). Poly-A modification and first-strand complementary DNA synthesis were performed with 1000 ng total RNA using the Mir-X miRNA First-Strand Synthesis Kit (TaKaRa, Tokyo, Japan) according to the manufacturer's instructions for the reverse-transcription reactions of miRNA. Quantitative PCR was performed on the Applied Biosystems Vii7 platform using SYBR Green Master Mix (Low Rox Plus; YEASEN, Shanghai, China) for messenger RNA or SYBR Premix Ex Taq II (TaKaRa, Tokyo, Japan) for small RNA (sRNA). Primer sequences are summarized in Table 3. All primer specificities were confirmed by dissociation curves using Vii7 system SDS software (Applied Biosystems by Life Technologies, Austin, TX). Ribosomal Protein S18 or U6 was used as the internal control.

Western Blot Analysis

Protein levels of PPAR α in rat liver tissues and cell lines (Huh7 and HepG2) were determined by Western blot analysis. Briefly, proteins were subjected to 10% sodium dodecyl sulfate–polyacrylamide gel electrophoresis and electroblotted to nitrocellulose membranes. PPAR α polyclonal antibody (ABclonal, Wuhan, China) and glyceraldehyde-3-phosphate dehydrogenase monoclonal antibody (Cell Signaling Technology, Boston, MA) were used as primary antibodies. Horseradish-peroxidase-conjugated

Table 3. Primer Sequences for Quantitative PCR

Gene name	Forward sequence	Reverse sequence
Rat		
<i>Ass1</i>	CACAGCACATCCTTGGACCTCTTC	AAGCGTTCTCCACGATGTCAATG
<i>p47phox</i>	GCCCAAAGATGGCAAGAATA	ATGACCTCAATGGCTTCACC
<i>p22phox</i>	GTAGATGCCGCTCGCAATGGCCAG	ATGGGGCAGATCGAGTGGCCATGT
<i>p67phox</i>	AGCAGAAGAGCAGTTAGCATTGG	TGCTTTCCATGGCCTTGTGTC
<i>Tnf</i>	TGCCTCAGCCTCTTCTCATT	GAGCCATTGGGAACCTTCT
<i>Il6</i>	AGTTGCCTTCTTGGGACTGA	CCTCCGACTTGTGAAGTGGT
<i>Il1b</i>	GAAGTCAAGACCAAGTGG	TGAAGTCAACTATGTCCCG
<i>Ccl2</i>	AGAATCACCAGCAGCAAGTGTC	TTGCTTGTCCAGGTGGTCCATG
<i>Ccr2</i>	CACCGTATGACTATGATGATG	CAGGAGAGCAGGTGAGAGAT
<i>Acta2</i>	TGTGCTATGTCGCTCTGGAC	CCAATGAAAGATGGCTG GAA
<i>Srebp1c</i>	CCAGCCTTTGAGGATAACCA	TGCAGGTCAGACACAGGAAG
<i>Scd</i>	AGCTGGTGATGTTCCAGAGG	CAAGAAGGTGCTGACGAACA
<i>Fasn</i>	GCCTAACACCTCTGTGCAGT	GGCAATACCCGTTCCCTGAA
<i>Acc</i>	GAATATCCAGATGGCCGAGA	CCTTCTGCTTGGCAAGTTC
<i>Ppara</i>	AATGCAATCCGTTTTGGAAG	TTGGCCAGAGATTTGAGGTC
<i>Pparg</i>	ACAAGAGCTGACCCAATGGT	GGCTCTTCATGTGGCCTGTT
<i>Cpt1α</i>	CCACGAAGCCCTCAAACAGA	CACACCCACCACCACGATAA
<i>Fabp1</i>	GTCTGCCTGAGGACCTCATCCAG	TCATGGTCTCCAGTTCGCACTCC
<i>Acadl</i>	ACTCCGCCTCCGCTTCCATG	TACCACCGTAGATCGGCTGAACTC
<i>Acadvl</i>	TTGGAGAAGGTGGAGGAGACAC	CTCTGCCAAGCGAGCGTACTG
<i>Acsl1</i>	ATGCCAGAGCTGATTGACATTCGG	CAAGGACTGCTGATCTTCGGACAC
<i>Fatp2</i>	CACGACAGAGTTGGAGACACCTTC	CCGATGCGACCTTCATGACCTG
Human and bacteria		
<i>PPARA</i>	ACGATTCGACTCAAGCTGGT	GTTGTGTGACATCCCACAG
<i>E fergusonii</i>	AGATTCACGTAAGCTGTTACCTT	CGTCTGATGAAAGATTTGGGAAG

anti-rabbit IgG (Beyotime, Shanghai China) was used as the secondary antibody. Immune complexes were detected using a Western chemiluminescent horseradish-peroxidase substrate (Millipore Corporation, Billerica, MA). Densitometry of immunoblot analysis was performed using ImageJ software (National Institutes of Health, Bethesda, MD).

sRNA High-Throughput Sequencing of E fergusonii

RNA sequencing, high-throughput sequencing, and subsequent bioinformatics analysis were performed by Cloud-Seq Biotech (Shanghai, China). One microgram of total RNA extracted from *E fergusonii* was treated with Antarctic phosphatase (New England Biolabs, Ipswich, MA) and polynucleotide kinase (PNK) enzyme (New England Biolabs). The RNA library was prepared according to the manufacturer's instructions for the TruSeq Small RNA Kit (Illumina, San Diego, CA). The libraries were size-selected for the sRNA fraction (137–170 nt) with 15% Tris-Borate-EDTA (TBE) polyacrylamide gel. Paired-end reads were harvested from an Illumina HiSeq 4000 sequencer and quality controlled by Q30. After 3' adaptor trimming, low-quality reads were removed with cutadapt software (v1.9.3).²⁶ sRNA candidates are predicted using an sRNA scanner based on transcriptional signals. sRNAs overlapping with known genes were excluded, and the rest were added to the gene annotation of the genome. The clean reads were aligned to the reference genome using Hisat2 software.²⁷ HTSeq was used to count the read numbers mapped to each gene.²⁸ edgeR was used to normalize the read counts

for each library.²⁹ Sequence data are available in the NCBI SRA with BioProject PRJNA747160.

Bacterial DNA Extraction and 16S rRNA Sequencing

For healthy controls and NAFLD patients, DNA was extracted from fecal samples. V3/V5 hypervariable regions of the 16S rDNA gene were amplified and sequenced on the 454 GS-FLX platform (Roche, Branford, CT) as previously described.¹⁸ For rats, total genomic DNA from fecal samples was extracted using a DNA Extraction Kit according to the manufacturer's instructions. The V3–V4 region of the 16S rRNA gene was amplified, purified, and sequenced on an Illumina MiSeq Platform (Illumina). Paired-end reads were processed using Trimmomatic software to detect and cut off ambiguous bases.³⁰ After trimming, paired-end reads were assembled using FLASH software.³¹ Reads with 75% of bases above Q20 were retained, and reads with chimeras were detected and removed using QIIME software (version 1.8.0).³² Clean reads were subjected to primer sequence removal and clustering to generate operational taxonomic units using Vsearch software with a 97% similarity cut-off level.³³ The representative read of each operational taxonomic unit was selected using the QIIME package. All representative reads were annotated and blasted against the Silva database using the ribosomal database project (RDP) classifier (confidence threshold, 70%).³⁴ The metabolic function of the gut microbiota was analyzed using Phylogenetic Investigation of Communities by Reconstruction of Unobserved States.³⁵ Sequence data were registered

at NCBI under BioProject PRJNA746446 (rats) and PRJNA747151 (human beings).

Cell Culture and sRNA Mimic Transfection

Huh7 and HepG2 cell lines were obtained from the American Type Culture Collection (ATCC, Manassas, VA). Dulbecco's modified Eagle medium supplemented with 10% fetal bovine serum (Gibco by Invitrogen, Carlsbad, CA) was used to culture cells under an atmosphere of 5% CO₂ at 37°C. Palmitic acid powder (Sigma-Aldrich, St. Louis, MO) was dissolved in 1% fatty acid-free bovine serum albumin at 65°C and filtered through a 0.22- μ m filter at a concentration of 5 mmol/L. The final concentration of palmitic acid used for experiments was 0.3 mmol/L. Huh7 or HepG2 cells were transfected with 50 nmol/L msRNA 23487 mimic or NC (RiboBio, Guangzhou, China) by Lipofectamine 3000 in Opti-MEM (Gibco) according to the manufacturer's instructions. Experiments were performed 24 hours after transfection.

Statistical Analysis

Results are expressed as the means \pm SEM. Statistical analysis was performed using analysis of variance and Student–Newman–Keuls multiple-range tests. Differences were considered significant at $P < .05$. Linear discriminant effect-size analysis was performed to determine the features most likely to account for differences between groups.³⁶

References

1. Wong RJ, Aguilar M, Cheung R, Perumpail RB, Harrison SA, Younossi ZM, Ahmed A. Nonalcoholic steatohepatitis is the second leading etiology of liver disease among adults awaiting liver transplantation in the United States. *Gastroenterology* 2015;148:547–555.
2. Diehl AM, Day C. Cause, pathogenesis, and treatment of nonalcoholic steatohepatitis. *N Engl J Med* 2017; 377:2063–2072.
3. Kim D, Kim WR. Nonobese fatty liver disease. *Clin Gastroenterol Hepatol* 2017;15:474–485.
4. Das K, Das K, Mukherjee PS, Ghosh A, Ghosh S, Mridha AR, Dhibar T, Bhattacharya B, Bhattacharya D, Manna B, Dhali GK, Santra A, Chowdhury A. Nonobese population in a developing country has a high prevalence of nonalcoholic fatty liver and significant liver disease. *Hepatology* 2010;51:1593–1602.
5. Cusi K. Nonalcoholic steatohepatitis in nonobese patients: not so different after all. *Hepatology* 2017;65:4–7.
6. Sharpton SR, Schnabl B, Knight R, Loomba R. Current concepts, opportunities, and challenges of gut microbiome-based personalized medicine in nonalcoholic fatty liver disease. *Cell Metab* 2021;33:21–32.
7. Zhou D, Pan Q, Xin FZ, Zhang RN, He CX, Chen GY, Liu C, Chen YW, Fan JG. Sodium butyrate attenuates high-fat diet-induced steatohepatitis in mice by improving gut microbiota and gastrointestinal barrier. *World J Gastroenterol* 2017;23:60–75.
8. Zhu L, Baker SS, Gill C, Liu W, Alkhouri R, Baker RD, Gill SR. Characterization of gut microbiomes in nonalcoholic steatohepatitis (NASH) patients: a connection between endogenous alcohol and NASH. *Hepatology* 2013;57:601–609.
9. Ghosal A, Upadhyaya BB, Fritz JV, Heintz-Buschart A, Desai MS, Yusuf D, Huang D, Baumuratov A, Wang K, Galas D, Wilmes P. The extracellular RNA complement of *Escherichia coli*. *Microbiologyopen* 2015;4:252–266.
10. Gaastra W, Kusters JG, van Duijkeren E, Lipman LJ. *Escherichia fergusonii*. *Vet Microbiol* 2014;172:7–12.
11. Buzzetti E, Pinzani M, Tsochatzis EA. The multiple-hit pathogenesis of non-alcoholic fatty liver disease (NAFLD). *Metabolism* 2016;65:1038–1048.
12. Liss KH, Finck BN. PPARs and nonalcoholic fatty liver disease. *Biochimie* 2017;136:65–74.
13. Watkins D, Arya DP. Regulatory roles of small RNAs in prokaryotes: parallels and contrast with eukaryotic miRNA. *Non-coding RNA Investig* 2019;3:28.
14. Betel D, Koppal A, Agius P, Sander C, Leslie C. Comprehensive modeling of microRNA targets predicts functional non-conserved and non-canonical sites. *Genome Biol* 2010;11:R90.
15. Bäckhed F, Ley RE, Sonnenburg JL, Peterson DA, Gordon JL. Host-bacterial mutualism in the human intestine. *Science* 2005;307:1915–1920.
16. Qian M, Hu H, Zhao D, Wang S, Pan C, Duan X, Gao Y, Liu J, Zhang Y, Yang S, Qi L-W, Wang L. Coordinated changes of gut microbiome and lipidome differentiates nonalcoholic steatohepatitis (NASH) from isolated steatosis. *Liver Int* 2020;40:622–637.
17. Mouzaki M, Comelli EM, Arendt BM, Bonengel J, Fung SK, Fischer SE, McGilvray ID, Allard JP. Intestinal microbiota in patients with nonalcoholic fatty liver disease. *Hepatology* 2013;58:120–127.
18. Shen F, Zheng R-D, Sun X-Q, Ding W-J, Wang X-Y, Fan J-G. Gut microbiota dysbiosis in patients with non-alcoholic fatty liver disease. *Hepatobiliary Pancreat Dis Int* 2017;16:375–381.
19. Farmer JJ 3rd, Fanning GR, Davis BR, O'Hara CM, Riddle C, Hickman-Brenner FW, Asbury MA, Lowery VA 3rd, Brenner DJ. *Escherichia fergusonii* and *Enterobacter taylorae*, two new species of Enterobacteriaceae isolated from clinical specimens. *J Clin Microbiol* 1985;21:77–81.
20. Lawrence JG, Ochman H, Hartl DL. Molecular and evolutionary relationships among enteric bacteria. *J Gen Microbiol* 1991;137:1911–1921.
21. Kang SM, Choi JW, Lee Y, Hong SH, Lee HJ. Identification of microRNA-size, small RNAs in *Escherichia coli*. *Curr Microbiol* 2013;67:609–613.
22. Johnson JS, Spakowicz DJ, Hong BY, Petersen LM, Demkowicz P, Chen L, Leopold SR, Hanson BM, Agresta HO, Gerstein M, Sodergren E, Weinstock GM. Evaluation of 16S rRNA gene sequencing for species and strain-level microbiome analysis. *Nat Commun* 2019; 10:5029.
23. Tu LN, Showalter MR, Cajka T, Fan S, Pillai VV, Fiehn O, Selvaraj V. Metabolomic characteristics of cholesterol-induced non-obese nonalcoholic fatty liver disease in mice. *Sci Rep* 2017;7:6120.

24. Chen C, Lu FC. The guidelines for prevention and control of overweight and obesity in Chinese adults. *Biomed Environ Sci* 2004;17(Suppl):1–36.
25. Bedossa P, Poitou C, Veyrie N, Bouillot JL, Basdevant A, Paradis V, Tordjman J, Clement K. Histopathological algorithm and scoring system for evaluation of liver lesions in morbidly obese patients. *Hepatology* 2012; 56:1751–1759.
26. Martin M. Cutadapt removes adapter sequences from high-throughput sequencing reads. *EMBnet J* 2011; 17:1–10.
27. Kim D, Paggi JM, Park C, Bennett C, Salzberg SL. Graph-based genome alignment and genotyping with HISAT2 and HISAT-genotype. *Nat Biotechnol* 2019; 37:907–915.
28. Anders S, Pyl PT, Huber W. HTSeq—a Python framework to work with high-throughput sequencing data. *Bioinformatics* 2015;31:166–169.
29. Robinson MD, McCarthy DJ, Smyth GK. edgeR: a Bioconductor package for differential expression analysis of digital gene expression data. *Bioinformatics* 2010; 26:139–140.
30. Bolger AM, Lohse M, Usadel B. Trimmomatic: a flexible trimmer for Illumina sequence data. *Bioinformatics* 2014; 30:2114–2120.
31. Reyon D, Tsai SQ, Khayter C, Foden JA, Sander JD, Joung JK. FLASH assembly of TALENs for high-throughput genome editing. *Nat Biotechnol* 2012; 30:460–465.
32. Caporaso JG, Kuczynski J, Stombaugh J, Bittinger K, Bushman FD, Costello EK, Fierer N, Peña AG, Goodrich JK, Gordon JL, Huttley GA, Kelley ST, Knights D, Koenig JE, Ley RE, Lozupone CA, McDonald D, Muegge BD, Pirrung M, Reeder J, Sevinsky JR, Tumbaugh PJ, Walters WA, Widmann J, Yatsunenkov T, Zaneveld J, Knight R. QIIME allows analysis of high-throughput community sequencing data. *Nat Methods* 2010;7:335–336.
33. Edgar RC, Haas BJ, Clemente JC, Quince C, Knight R. UCHIME improves sensitivity and speed of chimera detection. *Bioinformatics* 2011;27:2194–2200.
34. Wang Q, Garrity GM, Tiedje JM, Cole JR. Naive Bayesian classifier for rapid assignment of rRNA sequences into the new bacterial taxonomy. *Appl Environ Microbiol* 2007;73:5261–5267.
35. Langille MG, Zaneveld J, Caporaso JG, McDonald D, Knights D, Reyes JA, Clemente JC, Burkpile DE, Vega Thurber RL, Knight R, Beiko RG, Huttenhower C. Predictive functional profiling of microbial communities using 16S rRNA marker gene sequences. *Nat Biotechnol* 2013;31:814–821.
36. Segata N, Izard J, Waldron L, Gevers D, Miropolsky L, Garrett WS, Huttenhower C. Metagenomic biomarker discovery and explanation. *Genome Biol* 2011;12:R60.

Received August 5, 2021. Accepted December 3, 2021.

Correspondence

Address correspondence to: Jian-Gao Fan, MD, PhD, Department of Gastroenterology, Xinhua Hospital, School of Medicine, Shanghai Jiao Tong University, Shanghai Key Lab of Pediatric Gastroenterology and Nutrition, 1665 Kong Jiang Road, Shanghai, China 200092. e-mail: fanjiangao@xinhuaumed.com.cn; fax: (+86)-021-25077345; or Lu Jiang, PhD, Department of Pediatric Surgery, Xinhua Hospital, School of Medicine, Shanghai Jiao Tong University, Shanghai Institute for Pediatric Research; Shanghai Key Laboratory of Pediatric Gastroenterology and Nutrition, 1665 Kong Jiang Road, Shanghai, China 200092. e-mail: jianglu@xinhuaumed.com.cn; fax: (+86)-021-65791316.

Acknowledgments

The authors want to thank Lian Li and Jia-lin Yu (Oebiotech, China) for the gut microbiome analysis; Zhi-cai Yu, Nan-nan Zheng, and Dai-xi Jiang for their help with molecular biology experiments; as well as Dr Wei Cai for providing an excellent experimental platform and guidance.

CRedit Authorship Contributions

Feng-Zhi Xin (Data curation: Lead; Formal analysis: Lead; Writing – original draft: Lead)

Ze-Hua Zhao (Investigation: Equal; Methodology: Equal)

Xiao-Lin Liu (Investigation: Equal; Methodology: Equal)

Qin Pan (Investigation: Supporting)

Zi-Xuan Wang (Investigation: Supporting)

Lin Zeng (Data curation: Equal)

Qian-Ren Zhang (Methodology: Equal)

Lin Ye (Methodology: Equal)

Meng-Yu Wang (Methodology: Equal)

Rui-Nan Zhang (Investigation: Supporting)

Zi-Zhen Gong (Resources: Equal)

Lei-Jie Huang (Methodology: Equal)

Chao Sun (Resources: Equal)

Feng Shen (Resources: Equal)

Lu Jiang (Conceptualization: Equal; Investigation: Equal; Writing – review & editing: Lead)

Jian-Gao Fan, MD (Conceptualization: Lead; Project administration: Lead; Supervision: Lead; Writing – review & editing: Equal)

Conflicts of interest

The authors disclose no conflicts.

Funding

This study was supported by the National Key R&D Program of China (2017YFC0908903), and the National Natural Science Foundation of China (81873565, 81470840, and 81700503).